iScience

CellPress
OPEN ACCESS

Article

Dehydrated *Drosophila melanogaster* track a water plume in tethered flight

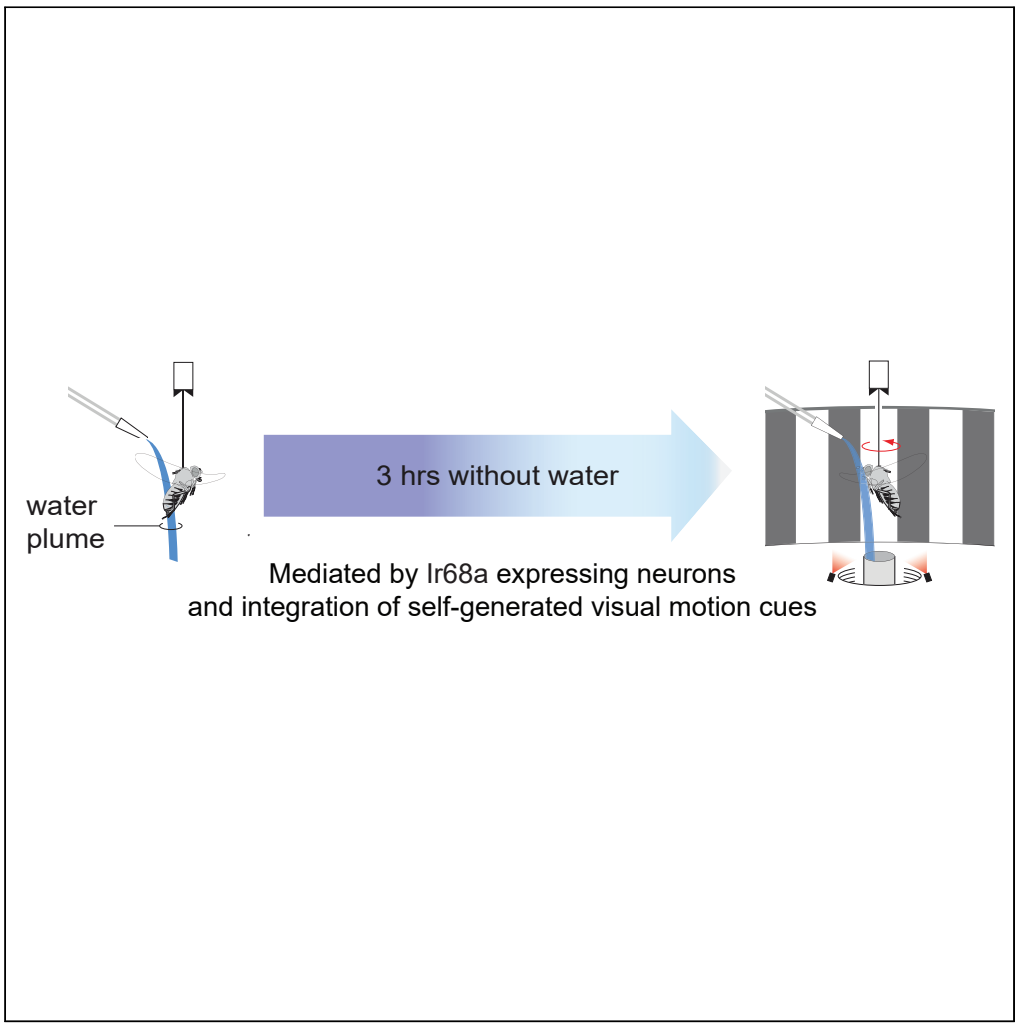

Daniela Limbania, Grace Lynn Turner, Sara M. Wasserman

swasserm@wellesley.edu

Highlights

Acute dehydration elicits water plume tracking in tethered flight

Self-generated visual motion cues are needed to stabilize and maintain water tracking

Water tracking requires functional a3 antennal segments

Water tracking requires Ir68a-expressing moist detecting neurons, but not *Orco*

Limbania et al., iScience *26*, 106266
March 17, 2023
https://doi.org/10.1016/j.isci.2023.106266

iScience

CellPress
OPEN ACCESS

Article

Dehydrated *Drosophila melanogaster* track a water plume in tethered flight

Daniela Limbania,[1] Grace Lynn Turner,[2] and Sara M. Wasserman[2,3,*]

SUMMARY

Perception of sensory stimuli can be modulated by changes in internal state to drive contextually appropriate behavior. For example, dehydration is a threat to terrestrial animals, especially to *Drosophila melanogaster* due to their large surface area to volume ratio, particularly under the energy demands of flight. While hydrated *D. melanogaster* avoid water cues, while walking, dehydration leads to water-seeking behavior. We show that in tethered flight, hydrated flies ignore a water stimulus, whereas dehydrated flies track a water plume. Antennal occlusions eliminate odor and water plume tracking, whereas inactivation of moist sensing neurons in the antennae disrupts water tracking only upon starvation and dehydration. Elimination of the olfactory coreceptor eradicates odor tracking while leaving water-seeking behavior intact in dehydrated flies. Our results suggest that while similar hygrosensory receptors may be used for walking and in-flight hygrotaxis, the temporal dynamics of modulating the perception of water vary with behavioral state.

INTRODUCTION

Here we examine the in-flight behavior of *Drosophila melanogaster* to moisture cues (hygrotaxis) using a flight simulator that suspends a tethered fly within a magnetic field, allowing the fly to rotate freely in the yaw plane (Figure 1A). In the remainder of the text, all references to flight indicate tethered flight, unless otherwise noted. The heading angle of the fly is measured in response to visual stimuli displayed on the surrounding LEDs and odor or water cues. An oscillating vertical bar is used to orient flies to a position 90 from a narrow odor or water plume delivered via low-flow air injected into water or apple cider vinegar (ACV). Headspace from each test tube is presented into the flight simulator at 180° (Figure 1A, orange plume) above the head of the fly and pulled down and out of the arena by a vacuum placed under the fly[1,2] (Figure 1A and STAR Methods).

While previous studies show that fed and hydrated (FH) walking flies assign a negative value to and actively avoid humidity cues,[3,4] flying flies assign a neutral value to a water plume, demonstrated by evenly distributed heading orientations throughout the arena[5,6] (Figures 1B and 1I). However, FH flies use a spatial gradient to orient toward and suppress body saccades (turns) to maintain their heading in order to "track" an attractive odor plume, such as ACV[5,6] (Figures 1C, 1H, and 1I). This leads to a significantly higher probability of finding an individual FH fly tracking an ACV plume compared to a water plume (Figure 1H). Flies have also been shown to "anti-track" in order to avoid an aversive odor plume.[7] Thus, this flight simulator can capture continuous heading behavior that reflects whether an individual fly has assigned an aversive, neutral, or attractive valence to a stimulus.

While some external stimuli elicit an innate valence assignment independent of changing conditions, others can elicit a variety of values. This flexibility is crucial for driving behavior that supports survival, for an individual must be able to modify the value assigned to salient sensory cues to accommodate changing internal and external environments. For example, walking flies dehydrated for 5–6 h alter the valence assigned to humidity cues, causing them to no longer avoid water cues but rather to seek them out to avoid desiccation.[4,8,9] Here, we tested the hypothesis that water deprivation would alter the valence assigned to a humid air (water) plume, changing it from neutral to positive to promote in-flight hygrotaxis.

[1]Department of Integrative Biology and Physiology, University of California, Los Angeles, Los Angeles, CA 90095, USA

[2]Department of Neuroscience, Wellesley College, Wellesley, MA 02481, USA

[3]Lead contact

*Correspondence: swasserm@wellesley.edu

https://doi.org/10.1016/j.isci.2023.106266

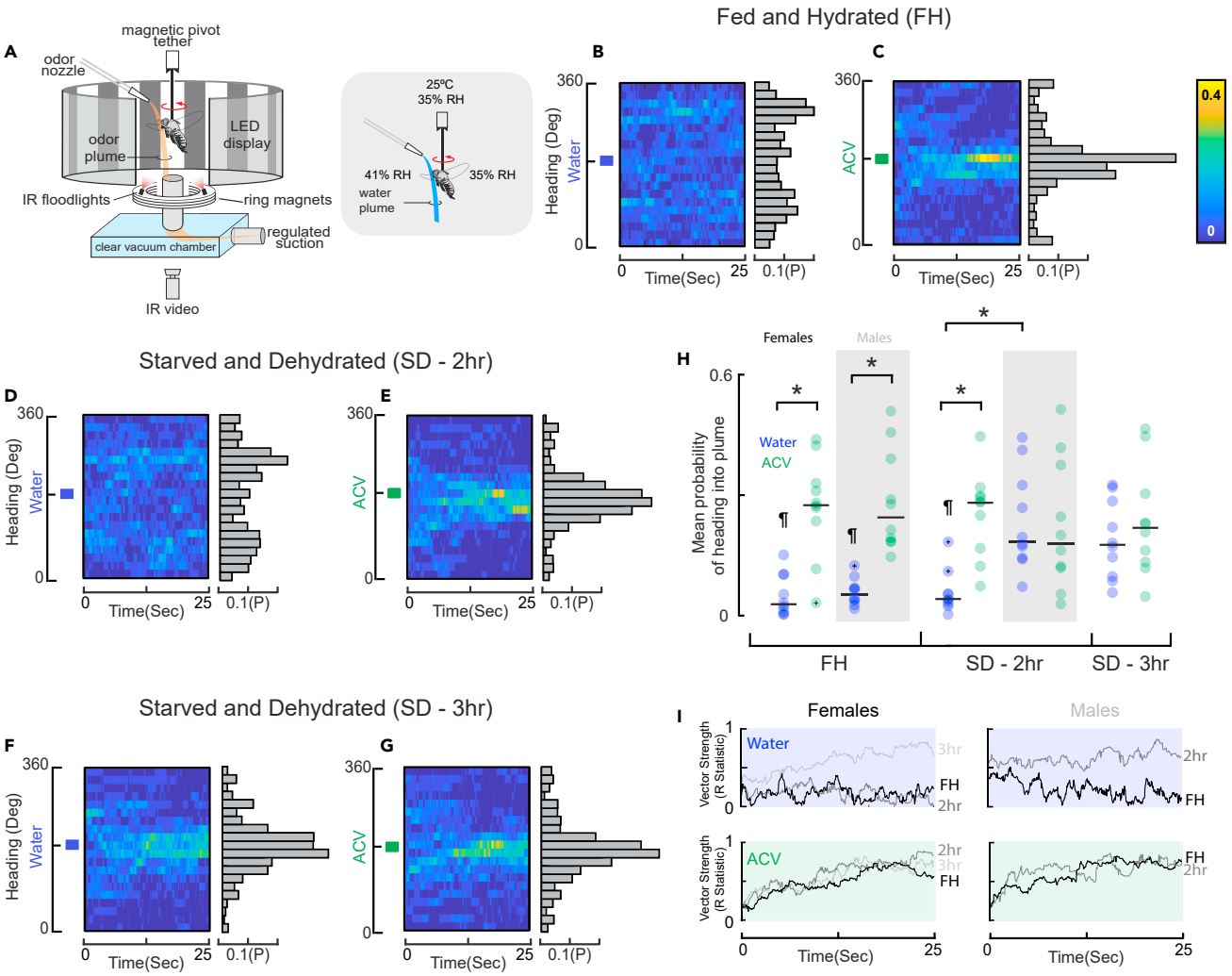

Figure 1. Water becomes an attractive stimulus to acutely starved and dehydrated flies in flight

(A) A fly is tethered to a pin and placed in a magnetic tether arena where it can freely rotate in the yaw plane. The fly is surrounded by panels of blue LED lights that can display high contrast stationary (*i.e.*, dark, and bright stripes as shown) or moving visual stimuli (*i.e.*, a rotating bar), used to visually drag and orient a fly to a particular starting point in the arena. An odor port is placed at 180° and delivers a narrow odor plume (shown in orange) or water (blue plume in gray inset box) that flows over the fly's head and is pulled down and out of the arena by a vacuum that sits beneath the fly. The relative humidity (RH) when the fly faces the water plume is 41% whereas orienting opposite the plume is 35% and measurements at the top and bottom of the arena also measure 35% RH. The average temperature in the arena measures 25°C. RH and temperature measurements of the room can be found in STAR Methods. Angular heading in response to varied plume and visual stimuli is recorded via infrared video and analyzed using custom written MATLAB code (see STAR Methods).

(B and C) Shown are heatmaps of heading trajectories of all individuals presented with a continuous odor plume of water or apple cider vinegar (ACV) and high contrast stripes displayed on the LED array. Heatmaps represent the probability of finding a fly with a particular angular heading over the duration of the experiment. Warmer colors (yellow) represent a higher probability with cooler colors (blue) a lower probability. Fed and Hydrated (FH) Wild-Type (WT) flies ignore a continuous water plume, indicated by a blue rectangle (B) and track a continuous apple cider vinegar (ACV) plume, indicated by a green rectangle (C) placed at 180°. A within-subjects design was used. Probability (P) histograms are shown in gray next to each heatmap with each bin representing 18° of the arena. N = 10 flies. Heading distributions between FH water and ACV conditions are significantly different from each other (Kolmogorov-Smirnov, p = 7.69E-24).

(D and E) WT flies removed from food and water for 2 h (SD - 2 h) ignore a continuous water plume (D) and track a continuous ACV plume with high contrast stripes displayed on the LED array (E). A within-subjects design was used with the set of flies from those described in B and C. N = 10 flies. Heatmaps and histograms are as described in B and C. Heading distributions between SD - 2 h water and ACV conditions are significantly different from each other (Kolmogorov-Smirnov, p = 6.39E-26). Heading distributions between FH (B) and SD - 2 h water (D) and between FH (C) and SD - 2 h ACV (E) conditions are not significantly different from each other (Kolmogorov-Smirnov, p = 0.69 and Kolmogorov-Smirnov, p = 0.24, respectively).

(F and G) WT flies removed from food and water for 3 h (SD - 3 h) track both a continuous water plume (F) and a continuous ACV plume with high contrast stripes displayed on the LED array (G). A within-subjects design was used with the same set of flies as those described in B–E. N = 10 flies. Heatmaps and histograms are as described in B and C. Heading distributions between SD - 3 h water and ACV conditions are still significantly different from each other but

Figure 1. *Continued*

to a much lower degree compared to FH and SD - 2 h conditions (Kolmogorov-Smirnov, p = 0.02). Heading distributions between SD - 2 h (D) and SD - 3 h water (F) and between SD - 2 h (E) and SD - 3 h ACV (G) conditions are significantly different from each other (Kolmogorov-Smirnov, p = 1.23E-19 and Kolmogorov-Smirnov, p = 0.003, respectively).

(H) Mean probability of finding individual female flies shown in heatmaps and histograms (Figures 1B–1G) and of male flies shown in heatmaps from Figure S1 heading into the water (blue dots) or ACV (green dots) plume from the last 20 s of the trial. Males are indicated by gray boxes. There are no males at SD - 3 h, as they were not able to complete the trials at this time point. Mean probability calculated over a minimum of two and maximum of three trials per fly. Blue indicates water plume and green indicates the ACV plume. Black bars represent group median and plus signs indicate outliers. Asterisks indicate $p < 0.005$ for shown comparisons and ¶ indicates $p < 0.005$ when compared to the starved and dehydrated 3 h water condition, via one-way ANOVA followed by Bonferroni's post hoc test.

(I) WT male and female starved and dehydrated for 2 and 3 h, respectively, track a water plume with the same robustness as an ACV plume. Shown is the vector strength of the mean heading position over time for the flies shown in the heatmaps (B–G). A vector strength closer to zero indicates high variance in the mean heading vector, whereas a vector strength closer to one indicates a mean heading vector with almost no variance. Female flies that are FH and starved and dehydrated for 2 h (2h) have variable heading throughout trials with a water plume (top left, blue rectangle, and vector strength close to zero), whereas female flies that have been starved and dehydrated for 3h (3h) have a mean heading vector with less variability (top left, blue rectangle and vector strength close to one). Male flies that are FH have variable heading throughout trials for a water plume (top right, blue rectangle, and vector strength close to zero), similar to FH and 2 h female flies. However, male flies that have been starved and dehydrated for only 2 h (2h) have a mean heading vector with less variability (top right, blue rectangle, and vector strength close to one), similar to the vector strength of 3 h female flies for a water plume. The mean heading vector for FH and SD (2h and 3h) in response to an ACV plume has less variability for both male and female flies (bottom, green rectangles, and vector strengths closer to one). See STAR Methods for vector strength calculations.

RESULTS AND DISCUSSION

Acutely starved and dehydrated flies track a water plume in flight

To test the temporal dynamics of hydration-dependent in-flight hygrotaxis, we removed female flies from food and water for 2 h and measured heading in response to a water or ACV plume presented in random order. We found that flies behaved similarly to FH flies, ignoring a water plume and tracking an ACV plume (Figures 1D, 1E, and 1H). However, after 3 h without food and water, the same flies tested in the FH and starved and dehydrated (SD - 2 h) conditions altered the value assigned to the water plume from neutral to attractive (Figures 1F–1H), and there was no significant difference in the probability of finding a fly orienting into the water plume compared to the ACV plume (Figure 1H). This suggested that upon 3 h of starvation and dehydration (SD), flies assign water the same highly positive value assigned to the food signal, ACV. Interestingly, likely due to their smaller size and decreased desiccation[10] and stress resistance,[11–13] males exhibit the switch to water plume tracking an hour earlier after water deprivationthan female flies (Figures 1H and S1). This apparent sexual dimorphism has also been observed in walking flies.[9] While we do not examine males further in this study, it will be interesting to examine the factors that contribute to the disparate temporal dynamics of state-dependent hygrotaxis in males and females.

To quantify tracking fidelity, we next calculated vector strength[14,15] across trials through the duration of the experiment. Although vector strength does not provide information about heading direction, a value closer to one indicates less variation in population heading direction whereas a measure closer to zero would indicate increased variation and less stability in flight heading. As expected, both FH and starved and dehydrated (SD - 2 h) flies ignore a water plume and turn about the arena and have a vector strength closer to zero; starved and dehydrated (SD - 3 h) flies that maintain heading into a water plume have a vector strength closer to one, similar to the vector strength for flies tracking ACV in all internal state conditions (Figure 1I).

Thirst alone is sufficient to induce water plume tracking in flight

Is in-flight hygrotaxis behavior due to dehydration, starvation, or both? Whereas laboratory flies obtain their food nutrients and water via the same medium, they have been shown to seek out and ingest water alone or obtain water from non-nutritional media.[16–18] We, therefore, investigated whether starvation alone would lead to water plume tracking by providing flies with non-nutritional (*e.g.*, no yeast or sugar) agarose for 3 h (3 h) (See STAR Methods). We again observed that FH flies ignore a water plume placed at 180° (Figures 2A and 2I), whereas flies that have been starved and dehydrated for 3 h (3 h) alter the value assigned to water and track a water plume with the same robustness as an ACV plume (Figures 2B and 2K). However, flies that were starved but hydrated (SH) no longer tracked a water plume (Figures 2C and 2M), demonstrating that the change in valence assigned to water is indeed due to dehydration and not starvation. No significant change was observed in the tracking of an ACV plume in all three internal state conditions (Figures 2D–2F, 2I, 2K, and 2M). Vector strength measurements for FH and SD flies once again reflected the change in valence assigned to water upon dehydration (Figures 1I, 2H, and 2J), and SH flies

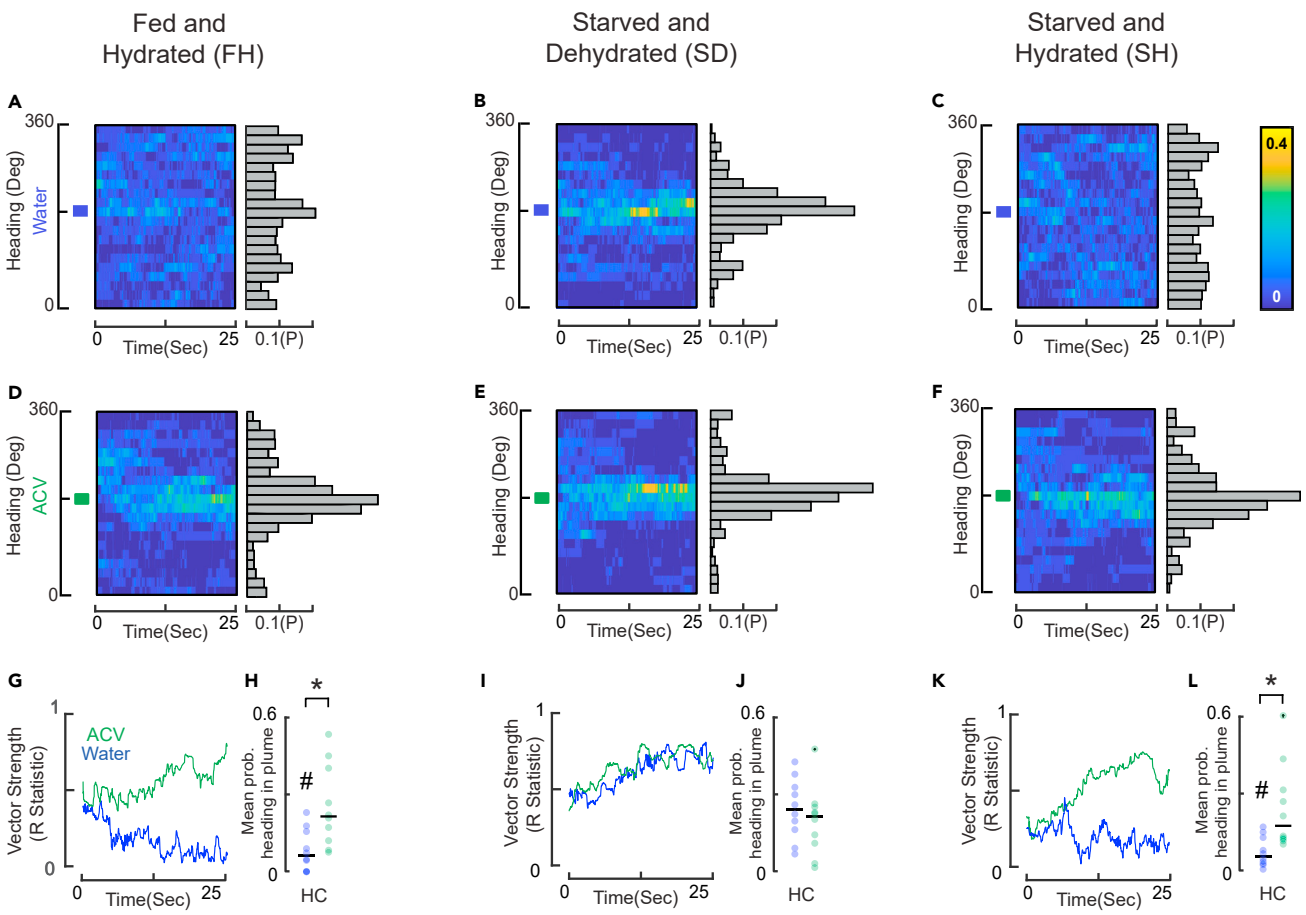

Figure 2. Acute dehydration alone is sufficient to make water attractive in flight

(A–F) Shown are heatmaps of heading trajectories of all individuals presented with a continuous odor plume of water or apple cider vinegar (ACV). Heatmaps represent the probability of finding a fly with a particular angular heading over the duration of the experiment. Warmer colors (yellow) represent a higher probability with cooler colors (blue) a lower probability. Tethered fed and hydrated (FH) Wild-Type (WT) flies ignore a continuous water plume in the magnetic tether arena (A). WT flies starved and dehydrated for 3 h (SD) track a water plume (B), and WT flies starved but hydrated for 3 h (SH) ignore a water plume (C). Fed and hydrated (D), starved and dehydrated (E), and starved and hydrated (F) flies track a continuous ACV plume. The placement of the water or ACV plume at 180° is indicated by a blue or green rectangle, respectively. Probability (P) histograms are shown in gray with each bin representing 18° of the arena. A within-subjects design was used within each internal state condition (*i.e.*, the same flies were observed for heading orientation to a water plume and ACV plume in the FH internal state condition) with a new set of flies used for each internal state condition. The heading distribution of SD flies presented with a water plume (B) is significantly different from heading distribution of FH water (A) and starved and hydrated (SH) water (C) (Kolmogorov-Smirnov, $p = 7.54E\text{-}22$ and $p = 2.39E\text{-}30$, respectively). FH water (A) and SH water (C) heading distributions are slightly significantly different from each other (Kolmogorov-Smirnov, $p = 0.03$). Heading distributions between FH water (A) and ACV (D) conditions are significantly different from each other (Kolmogorov-Smirnov, $p = 1.81E\text{-}13$). Heading distributions between SD water (B) and ACV (E) conditions are not significantly different from each other (Kolmogorov-Smirnov, $p = 0.05$). Heading distributions between SH water (C) and ACV (F) conditions are significantly different from each other (Kolmogorov-Smirnov, $p = 3.23E\text{-}25$). Heading distributions in response to an ACV plume are significantly different across internal state conditions (D–F: FH and SD Kolmogorov-Smirnov, $p = 8.35E\text{-}07$; SD and SH Kolmogorov-Smirnov, $p = 0.01$; FH and SH Kolmogorov-Smirnov, $p = 0.02$). (G, I, and K) Dehydration and not starvation leads to robust tracking of a water plume in tethered flight. Shown is the vector strength of the mean heading position over time for the flies shown in the corresponding heatmaps and histograms (A–F). Blue and green lines indicated the water and ACV plume conditions, respectively. (H, J, and L) Mean probability of finding individual flies heading into the water (blue dots) or ACV (green dots) plume from the last 20 s of the trial is shown in corresponding heatmaps and histograms (A–F). Mean probability calculated over a minimum of two and maximum of three trials per fly. Black bars represent group median and plus signs indicate outliers. Odor conditions were randomly presented to each individual fly and high-contrast stripes were displayed on the arena. Asterisks indicate $p < 0.005$ for shown comparisons, # indicates $p < 0.005$ when compared to SD flies in the same plume condition, via one-way ANOVA followed by Bonferroni's post hoc test. N = 10 flies.

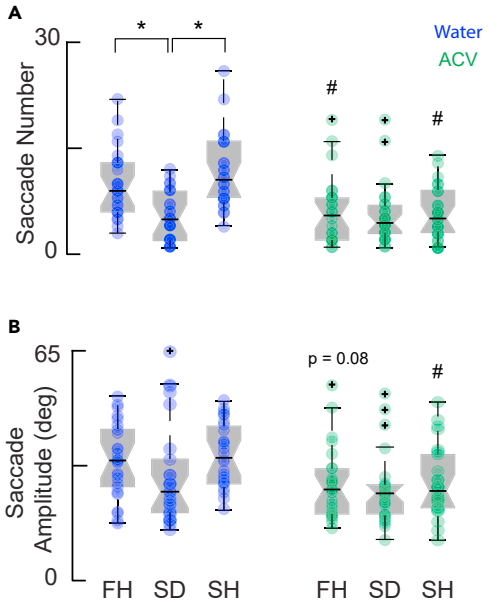

Figure 3. Dehydrated flies suppress saccade number and amplitude to maintain a stable heading in a water or ACV plume

(A) Mean saccade number across three internal states.
(B) Mean saccade amplitude across three internal states. Blue and green dots indicate mean saccade number (A) or mean saccade amplitude (B) per individual fly in the presence of a water or ACV plume, respectively. N = 10 flies. Boxplots indicate the 25th, 50th (median indicated by a black horizontal line), and 75th percentiles. Whiskers show the minimum and maximum saccade number (A) or amplitude (B). Outliers are indicated by plus signs. Asterisks indicate $p < 0.05$ for shown comparisons and # indicate $p < 0.05$ compared to water in the same internal state condition, via Mann-Whitney for (A) and via one-way ANOVA followed by Bonferroni's post hoc test for (B). N = the same 10 flies shown in Figure 2.

responded similarly to FH flies (Figure 2L). Vector strength measurements, once again, looked similar in response to an ACV plume across all three internal state conditions (Figures 2H, 2J, and 2L).

Flies navigate using both smooth and saccadic movements. Motor control of body saccades (rapid turns) allows for reorientation for search behavior while maintaining visual gaze stability.[19,20] Maintaining position within a continuous odor plume in tethered flight is in part mediated by the suppression of saccade rate and reduced amplitude,[5–7] and plume tracking in a more naturalistic free-flight scenario with variable wind conditions has revealed additional strategies.[21] As previously observed, FH flies reduce the number of body saccades as well as saccade amplitude in response to a discrete ACV plume, but not a water plume (Figure 3A, "FH").[5,6] We note that in FH flies, whereas suppression of saccade amplitude in response to ACV is not statistically significant compared to water (Figure 3B, "FH"), we see a similar trend as previously reported. However, upon acute SD, flies significantly reduce saccade number, to the same degree as when tracking an ACV plume, in order to track a water plume (Figure 3A, "SD"). The decrease in saccade rate is eliminated when flies are starved and hydrated (Figure 3A, "SH"), and thus suggests that dehydration alone is sufficient to lead to modulation of saccade number needed to maintain heading into a water plume. We did not observe any difference in saccade number when tracking an ACV plume in varied internal state conditions, suggesting that SD do not increase the salience of ACV or that the flies already maximally track the plume for the duration of the experiments in the FH condition. Additionally, we see a trend in saccade amplitude reduction in starved and dehydrated flies in response to a water plume (Figure 3B, "SD"), and saccade amplitude is not significantly different between water and ACV tracking upon SD. Thus, upon dehydration, flies utilize similar motor control of body saccades to track both ACV and water in flight.

Tracking a water plume in flight requires self-generated motion cues

Appetitive and aversive odor plume tracking both require the integration of self-generated motion cues for sustained stabilization within or away from the plume.[6,7] Do flies also require wide-field motion cues to stabilize their heading within a water plume when dehydrated? To test this, we starved flies for 3 h, then presented them with a water or ACV plume in a featureless uniformly lit arena (thus removing self-generated visual cues). As previously reported, removing visual cues disrupted ACV plume tracking, and we report a similar behavioral disruption to water plume tracking, leading to a significantly lower probability of finding a fly heading into both ACV and water plumes. This was also reflected by a lower vector strength, representative of a more variable heading (Figure S2). Upon dehydration, flies suppress saccade number, and to some extent, saccade amplitude in order to maintain heading within a water plume (Figure 3, Striped Condition). It would be interesting to investigate how flies adapt and switch their sensorimotor program to respond to the same stimulus with two different behavioral outcomes in a state-dependent manner.

Flies do not require a functional olfactory system to track a water plume when dehydrated

Mosquitoes are known to rely on hygrotaxis to locate standing water for oviposition.[22] Why would *D. melanogaster* need to be able to locate and stabilize heading to track a humid air plume? Flies are capable of maintaining heading and traveling great distances (about 12 km) with minimal visual cues to stabilize their trajectory to arrive at far-off oases.[23] One could imagine that the ability to integrate and utilize humidity gradients to localize food and water sources would be advantageous to survival. Hygrotaxis is mediated by both the detection of water vapor detected via receptors in the third antennal segment, and by water consumption, detected by distributed gustatory mechanisms. Do the receptors that mediate walking hygrotaxis also support in-flight hygrotaxis? In *D. melanogaster*, there is evidence for both mechanosensitive[3,24] and ionotropic receptors (IRs) playing a role in mediating hygrotaxis.[25–29] Hygrotaxis behavior in walking flies does not, however, rely on olfactory receptors (ORs),[24] and therefore, we reasoned that water plume tracking in-flight should occur independently of the functional status of olfactory receptors. *D. melanogaster* ORs rely upon an olfactory coreceptor (ORCO) to function. As such, we hypothesized that as has been previously shown, anosmic *Orco* mutants[30] would not track an ACV plume but would track a water plume after acute dehydration. Indeed, we observed that similar to FH Wild-Type (WT) flies, FH *Orco* flies do not track a water plume. *Orco* flies are not able to track an ACV plume when fed and hydrated (Figures 4A, 4B, and 4I–4J) but maintain their ability to track a water plume after acute dehydration (SD) (Figures 4C and 4I), while continuing to ignore an ACV plume (Figures 4D and 4J). Interestingly, while *Orco* flies show an increased probability of heading into a water plume upon SD (Figure 4I), they also showed a slight increase in the probability of heading into an ACV plume (Figure 4J, ORCO −/− "SD"). As Orco flies are anosmic and cannot smell ACV, we hypothesized that the slight increase in heading into the ACV plume was due to the water cues captured in the headspace of the ACV solution in the olfactometer. We tested this idea by repeating the experiment using ACV applied to a piece of filter paper to remove moisture cues.[7] These *Orco* mutants maintained their dehydration-dependent water plume tracking (Figures 4I and S2) but did not show an increase in their ACV tracking (Figure 4J, ORCO −/− ACV FP, "SD" and Figure S3). Recent work identified a mechanosensitive channel required for hygrotaxis housed within olfactory neurons. The authors propose that the spatial localization of the hygroreceptor in food odor-detecting neurons could underlie multimodal integration that supports food-seeking behavior.[24] Since water does not elicit in-flight hygrotaxis in hydrated flies but does so upon acute dehydration, this could provide a novel model for further exploring state-dependent multimodal integration.

Flies require functional antennae and Ir68a-expressing moist detecting neurons to track a water plume when dehydrated

Having confirmed that in-flight state-dependent tracking of a water plume operates independently from ORs, we next asked whether IRs housed in the sacculus, an invagination on the third (a3) antennal segment previously shown to mediate walking hygrotaxis behavior[25–28] also mediate in-flight water tracking behavior. Blocking the a3 segment by painting UV-activated glue on the a3 segment to block odor receptors is known to eliminate tracking of attractive odors.[5,31] We painted UV-activated glue on the a3 segment to block both ACV-sensing ORs as well as the sacculus containing previously identified hygroreceptors and hygrosensory neurons. We did not observe water or ACV tracking in any internal state (Figures 4E–4H and 4I–4J) confirming that state-dependent water plume tracking does not rely on ORs but likely does rely on hygrosensory receptors housed on the third antennal segment, as has been previously reported to underlie water seeking behavior in walking flies after longer-term water deprivation.[25–29] This result also rules out the possibility that in-flight water plume tracking relies on appetitive gustatory signals, mediated by mechanisms outside of the a3 antennal segment. We note that, as expected, *Orco* and AO flies all track ACV significantly less than WT flies, however, they also track water significantly less in the SD state, compared to WT. We often see less robust behavior overall in mutants and manipulated animals and are confident that while the water plume tracking is not as robust as WT, it is still significantly greater than the internal FH control within each line. Additionally, this perhaps points to multimodal integration of water and odor cues at the level of sensation[24] because water likely contains some odor signals that work in combination with an increased salience of water leading to an even greater probability of orienting into a water plume in a dehydrated state.

We next examined whether Ir68a-expressing moist detecting neurons housed in the sacculus, previously identified as mediating walking hygrotaxis,[26] were also required for in-flight hygrotaxis behavior. We silenced Ir68a-expressing neurons by expressing the inward rectifying channel, Kir under Ir68a-Gal4, and found that indeed, these flies were no longer able to stabilize their heading to track a water plume upon

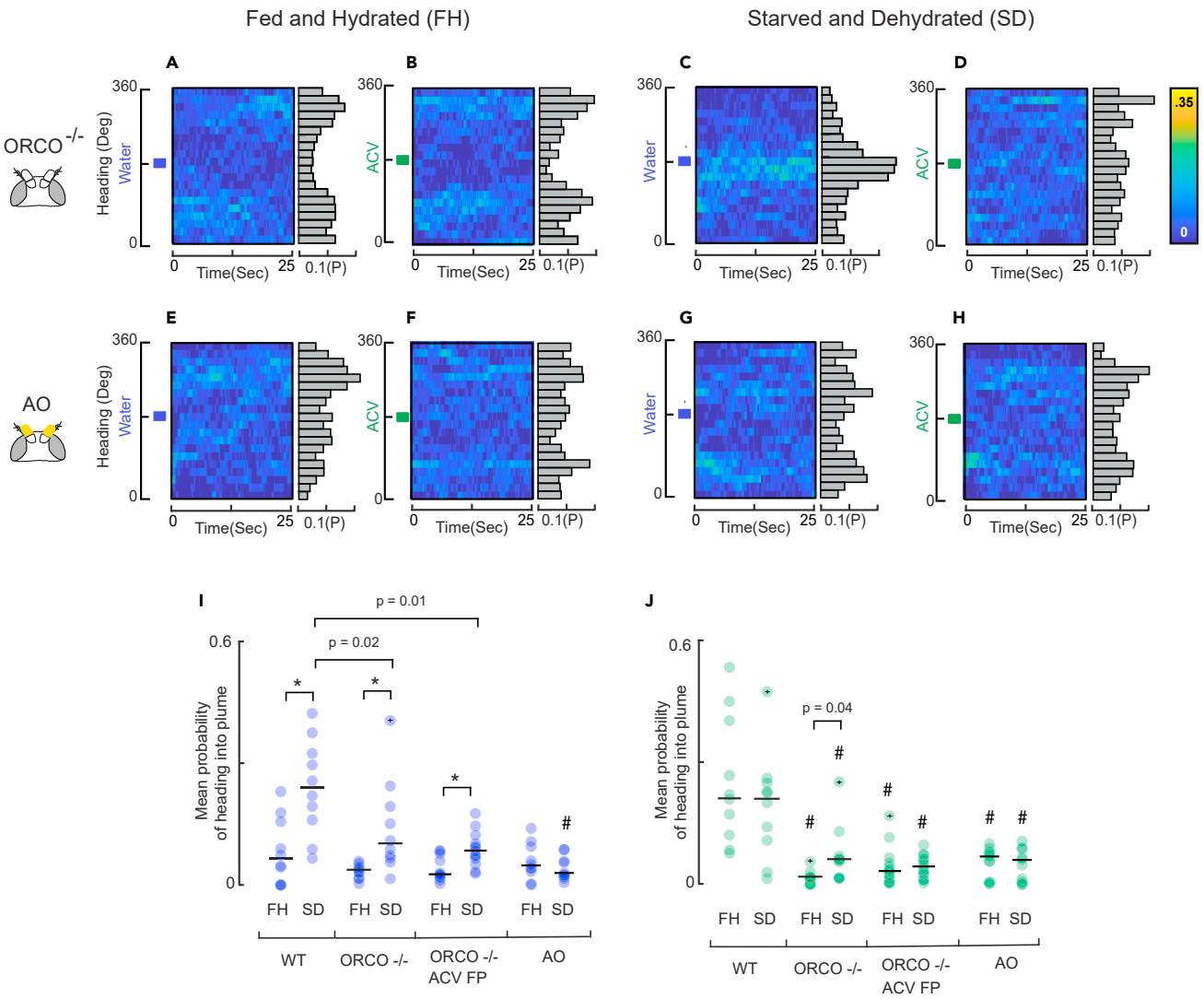

Figure 4. Flies require functional antennae but not a functional olfactory system to track a water plume When dehydrated

(A–H) Shown are heatmaps of heading trajectories of all individuals presented with a continuous odor plume at 180° of water (blue rectangle) or ACV (green rectangle). Heatmaps represent the probability of finding a fly with a particular angular heading over the duration of the experiment. Warmer colors (yellow) represent a higher probability with cooler colors (blue) a lower probability. Tethered *Orco* mutants (A–D) and tethered WT flies with occluded antennae (AO) (E–H) are not able to track a water or ACV plume when fed and hydrated (FH). Tethered *Orco* mutants do track water (C) when starved and dehydrated (SD) but do not track ACV (D). Tethered WT flies with occluded antennae (AO) do not track water (G) when starved and dehydrated (SD) and do not track ACV in either internal state condition (F and H). Antennae were occluded using UV-activated glue, highlighted in the figure in yellow (See STAR Methods).

Probability (P) histograms are shown in gray next to each heatmap with each bin representing 18° of the arena. Heading distributions for *Orco* flies: FH water (A) and ACV (B) conditions are not significantly different from each other (Kolmogorov-Smirnov, p = 0.22), while SD water (C) and ACV (D) conditions are significantly different from each other (Kolmogorov-Smirnov, p = 2.43E-07). Heading distributions between FH water (A) and SD Water (C) conditions are significantly different from each other (Kolmogorov-Smirnov, p = 7.03E-4). While there is a significant difference in heading distribution between FH ACV (B) and SD ACV (D) (Kolmogorov-Smirnov, p = 0.01) this seems to be due to an increased exploratory behavior, perhaps initiated by starvation. Heading distributions for AO flies: FH water (E) and ACV (F) conditions are significantly different from each other (Kolmogorov-Smirnov, p = 0.01), as are SD water (G) and ACV (H) conditions (Kolmogorov-Smirnov, p = 9.99E-01). Heading distributions between FH water (E) and SD Water (G) conditions are significantly different from each other (Kolmogorov-Smirnov, p = 2.25E02). While heading distribution between FH ACV (F) and SD ACV (H) are not significantly different from one another (Kolmogorov-Smirnov, p = 0.75). Again, while some heading distributions are significantly different from one another, none reflect plume tracking behavior but rather differences in exploratory turning behaviors. N = 10 flies.

(I–J) Mean probability of finding individual flies heading into the water (I, blue dots) or ACV (J, green dots) plume shown in corresponding heatmaps and histograms (A–H) from the last 20 s of the trial. Mean probability calculated over a minimum of two and maximum of three trials per fly. Black bars represent group median and plus signs indicate outliers. Asterisks indicate $p < 0.05$ for shown comparisons and # indicates $p < 0.05$ when compared to WT flies in the same internal state and plume condition, via unpaired t-test. A within-subjects design was used for the *Orco* and AO flies. N = 13 *Orco* flies and N = 10 WT AO flies.

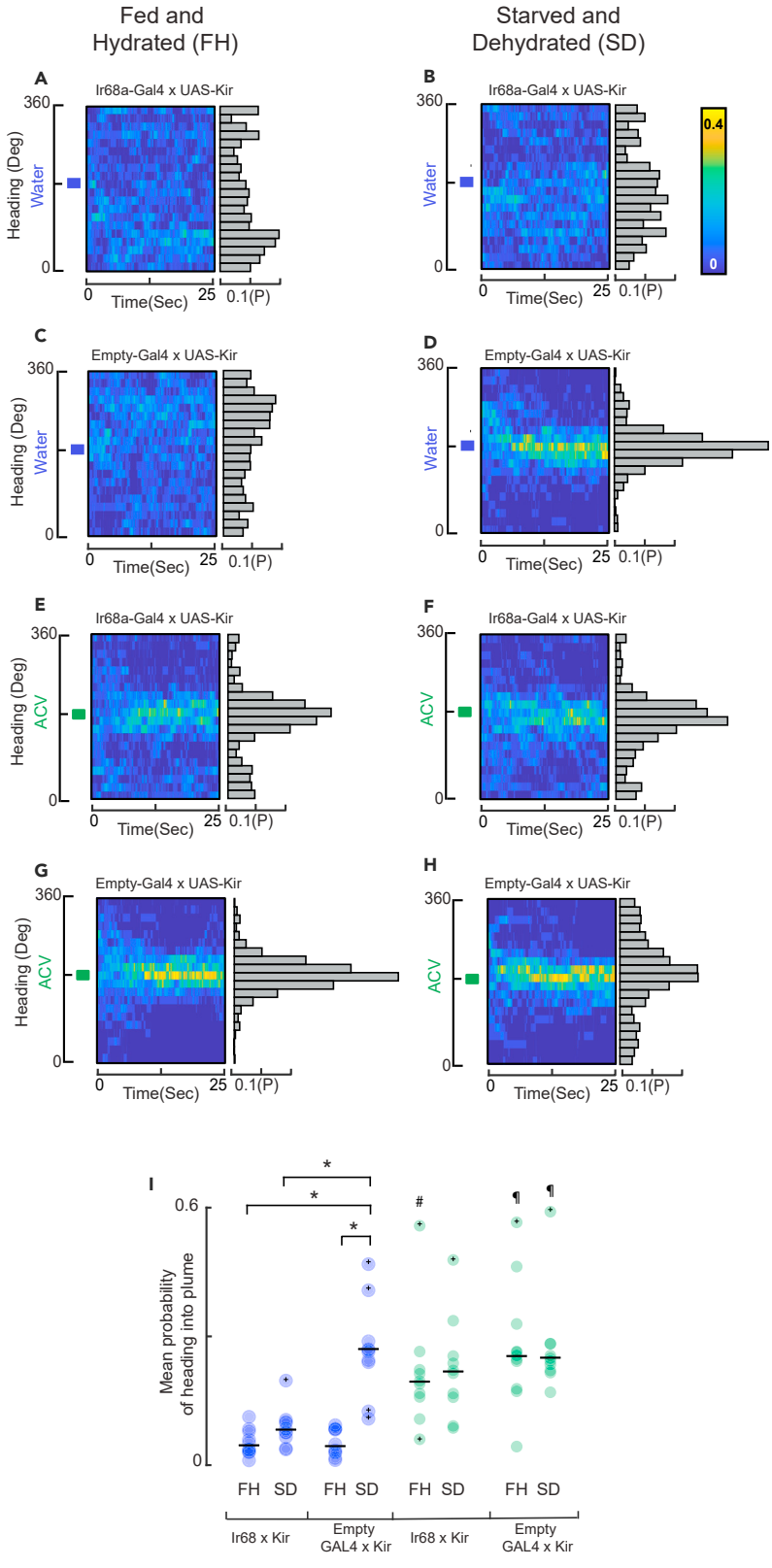
Fed and
Hydrated (FH)
Starved and
Dehydrated (SD)
A
Ir68a-Gal4 x UAS-Kir
B
Ir68a-Gal4 x UAS-Kir
C
Empty-Gal4 x UAS-Kir
D
Empty-Gal4 x UAS-Kir
E
Ir68a-Gal4 x UAS-Kir
F
Ir68a-Gal4 x UAS-Kir
G
Empty-Gal4 x UAS-Kir
H
Empty-Gal4 x UAS-Kir
Heading (Deg)
Water
ACV
360
0
0.4
Time(Sec)
25
0.1(P)
I
Mean probability
of heading into plume
0.6
FH SD FH SD FH SD FH SD
Ir68 x Kir
Empty
GAL4 x Kir
Ir68 x Kir
Empty
GAL4 x Kir

Figure 5. Flies require functional moist detecting neurons to track a water plume upon dehydration

(A–H) Shown are heatmaps of heading trajectories of all individuals presented with a continuous odor plume at 180° of water (blue rectangle) or ACV (green rectangle). Heatmaps represent the probability of finding a fly with a particular angular heading over the duration of the experiment. Warmer colors (yellow) represent a higher probability and cooler colors (blue) represent a lower probability. Fed and hydrated (FH) tethered Ir68a-GAL4 x Kir (A) and starved and dehydrated (SD) Ir68a-GAL4 x Kir (B) do not track a water plume. FH Control Empty-GAL4 x Kir do not track a water plume (C), yet SD Empty-GAL4 x Kir do track a water plume (D). FH and SD Ir68a-GAL4 x Kir (E and F, respectively) and FH and SD Control Empty-GAL4 x Kir (G and H, respectively) all track an ACV plume. Heading distributions for Ir68a-GAL4 x Kir flies: FH water (A) and ACV (E) conditions are significantly different from each other (Kolmogorov-Smirnov, p = 2.20E-19), as are SD water (B) and ACV (F) (Kolmogorov-Smirnov, p = 5.10E-14). Heading distributions between FH water (A) and SD Water (B) conditions are significantly different from each other (Kolmogorov-Smirnov, p = 6.17E-2) as are heading distributions between FH ACV (E) and SD ACV (F) conditions (Kolmogorov-Smirnov, p = 0.03). Heading distributions for Empty-GAL4 x Kir: FH water (A) and ACV (E) conditions are significantly different from each other (Kolmogorov-Smirnov, p = 2.20E-19), as are SD water (B) and ACV (F) (Kolmogorov-Smirnov, p = 5.10E-14). FH water (C) and FH ACV (G) are significantly different from each other (Kolmogorov-Smirnov, p = 2.77E-54), while SD water (D) and SD ACV (H) are significantly different from one another (Kolmogorov-Smirnov, p = 2.72E-04). Heading distributions for Empty-GAL4 x Kir and Ir68a-GAL4 x Kir flies: FH Ir68a-GAL4 x Kir water (A) and FH Empty-GAL4 x Kir water (C) conditions are not significantly different from each other (Kolmogorov-Smirnov, p = 0.62). SD Ir68a-GAL4 x Kir water (B) and SD Empty-GAL4 x Kir water (D) conditions are significantly different from each other (Kolmogorov-Smirnov, p = 4.77E-30). FH Ir68a-GAL4 x Kir ACV (E) and FH Empty-GAL4 x Kir ACV (G) conditions are significantly different from each other (Kolmogorov-Smirnov, p = 1.39E-21). SD Ir68a-GAL4 x Kir ACV (F) and SD Empty-GAL4 x Kir ACV (H) conditions are significantly different from each other (Kolmogorov-Smirnov, p = 6.93E-18). N = 10 flies for each genotype.

(I) Mean probability of finding individual flies heading into the water (blue dots) or ACV (green dots) plume shown in corresponding heatmaps and histograms (A–H) from the last 20 s of the trial. Mean probability calculated over a minimum of two and maximum of three trials per fly. Black bars represent group median and plus signs indicate outliers. Asterisks indicate $p < 0.05$ for shown comparisons and # indicates $p < 0.05$ when compared to FH water plume conditions and ¶ indicates $p < 0.05$ when compared to all water plume conditions, except Empty-GAL4 x Kir SD, via one-way ANOVA followed by Bonferroni's post hoc test. A within-subjects design was used for the Ir68a-GAL4 x Kir and Empty-GAL4 x Kir flies. N = 10 flies.

dehydration (Figure 5A, 5B, and 5I). The expression of Kir under a control Empty-Gal4 did not disrupt water plume tracking upon dehydration (Figure 5C, 5D, and 5I). However, while Ir68a-Gal4 x UAS-Kir water tracking upon SD is significantly different from the Empty-Gal4 x Kir SD water plume tracking, we note that upon SD the mean probability of Ir68a-Gal4 x UAS-Kir orienting into a water plume is not significantly different from FH or SD ACV plume tracking (Figure 5I). This could be due to the somewhat less robust ACV tracking observed in Ir68a-Gal4 x UAS-Kir FH and SD ACV (Figure 5E, 5F, and 5I), which could be enhanced with the integration of moisture cues in flies with functional Ir68a-expressing neurons. Empty-Gal4 x Kir FH and SD flies robustly tracked an ACV plume (Figure 5G–5I). Hydrated flies have been shown to depend upon both moist and dry sensing neurons to mediate walking hygrotaxis behavior, while desiccated flies still exhibit walking hygrotaxis with either dry or moist sensing neurons inactivated 25. It is interesting that in-flight hygrotaxis is significantly disrupted when only moist-detecting neurons are inactivated, and it could be possible that the inactivation of both dry- and moist-sending neurons would lead to a more severe phenotype in flight. It is evident that Ir68a-expressing neurons contribute greatly to hydration state-dependent in-flight hygrotaxis behavior.

In summary, our findings show that *D. melanogaster* only track a water plume in-flight when dehydrated and that dehydration-dependent hygrotaxis occurs on a much faster timescale than previously shown in walking assays (Figure 1). Similar to walking flies, in-flight hygrotaxis does not require functional ORs as demonstrated by *Orco* flies tracking a water plume upon dehydration (Figure 4). However, flies do require functional antennae (Figure 4) and functional Ir68a-expressing moist cells (Figure 5) to support state-dependent hygrotaxis behavior. While there is evidence of moths and bees approaching flowers based on humidity cues in flight[32–35] to our knowledge, this is the first demonstration of sustained in-flight water plume tracking behavior and the first to show that in-flight hygrotaxis triggered only in response to thirst (no water consumption) rather than environmental desiccation.

These results set up a foundation to further explore the mechanisms by which changes in the internal state of the body are sensed and how these signals modulate state-dependent behavior. Neuromodulators have been shown to enable flexibility from within the neural circuits and computations required to generate adaptive behavior in different internal and behavioral states.[31,36–38] In particular, naive water seeking (*i.e.*, not learned) in walking flies is mediated by rewarding dopaminergic circuits.[4] In addition, ion transport

peptide (ITP), a protein hormone functionally analogous to vasopressin and the renin-angiotensin pathway has been recently shown to play a role in water storage and thirst in *D. melanogaster*,[39] critical for promoting water-seeking behavior. These are just a few examples of how the internal state conducts a coordinated effort between systems that operate on varied timescales and are spatially distributed across the body and brain (reviewed in[40]). The findings reported here provide a platform to further explore general principles of the spatiotemporal dynamics of interoception[41–43] and the neuromodulatory mechanisms that communicate internal state changes in sensory perception to generate behavior that supports survival.

Limitations of the study

Our study demonstrates that functional antennae but not the olfactory system are required for thirst-dependent hygrotaxis behavior in flight. Specifically, we show that the Ir68a-expressing moist sensing cells are required for in-flight state-dependent hygrotaxis behavior. The a3 segment houses additional IRs previously identified as playing a role in sensing both moist and dry air needed to drive hydration-state-dependent walking hygrotaxis. Future work investigating how combinations of these receptors work together in flight are needed. Additionally, previous studies have revealed that odor concentration can influence both free flight[21] and tethered flight[6] behavior. We measured the relative humidity (RH) at the top of the leaves of an exterior plant and compost pile around dusk and found RH levels of 62% with ambient RH of 55% and 54%, respectively. While the magnetic tether arena does not introduce an ethological wind feature to mimic more naturalistic odor plumes, future free flight studies and presentation of plumes with a range of humidity levels that represent humidity cues that ethological environmental features might emit will be exciting to further elucidate the range of state-dependent water plume tracking in tethered flight.

STAR★METHODS

Detailed methods are provided in the online version of this paper and include the following:

- KEY RESOURCES TABLE
- RESOURCE AVAILABILITY
  - Lead contact
  - Materials availability
  - Data and code availability
- EXPERIMENTAL MODEL AND SUBJECT DETAILS
- METHOD DETAILS
  - Magnetic tether flight simulator
- QUANTIFICATION AND STATISTICAL ANALYSIS

SUPPLEMENTAL INFORMATION

Supplemental information can be found online at https://doi.org/10.1016/j.isci.2023.106266.

ACKNOWLEDGMENTS

We thank Mark Frye and members of the Frye lab for providing research space, helpful discussion, and feedback, Gio Frighetto for sharing the code used to analyze heading trajectories and saccades dynamics, Paul Garrity for providing research space and *Orco* mutant flies, and Allie Salomon, Rachel Mernoff, and Austin Wang for preliminary troubleshooting and proof of concept experiments. Funding: National Science Foundation IOS-2016188 to S.W., Wellesley College Start-up to S.W., and Summer Research Funds to G.T.

AUTHOR CONTRIBUTIONS

D.L.: Data Collection and Validation, Analysis, Visualization, Curation, and Writing - original and revised draft.

G.T.: Review and Editing, and Preliminary Data Collection.

S.W.: Conceptualization, Methodology, Visualization, Writing, Supervision, and Funding acquisition.

DECLARATION OF INTERESTS

The authors declare no competing interests.

INCLUSION AND DIVERSITY

One or more of the authors of this paper self-identifies as an underrepresented ethnic minority in their field of research or within their geographical location. One or more of the authors of this paper self-identifies as a gender minority in their field of research. One or more of the authors of this paper self-identifies as a member of the LGBTQIA+ community. One or more of the authors of this paper self-identifies as living with a disability. We support inclusive, diverse, and equitable conduct of research.

Received: July 29, 2022
Revised: September 9, 2022
Accepted: February 17, 2023
Published: February 24, 2023

REFERENCES

1. Duistermars, B.J., and Frye, M.A. (2008). A magnetic tether system to investigate visual and olfactory mediated flight control in Drosophila. J. Vis. Exp. e1063. https://doi.org/10.3791/1063.

2. Duistermars, B.J., and Frye, M. a ((2008). Report crossmodal visual input for odor tracking during fly flight. Curr. Biol. *18*, 270–275. https://doi.org/10.1016/j.cub.2008.01.027.

3. Liu, L., Li, Y., Wang, R., Yin, C., Dong, Q., Hing, H., Kim, C., and Welsh, M.J. (2007). Drosophila hygrosensation requires the TRP channels water witch and nanchung. Nature *450*, 294–298. https://doi.org/10.1038/nature06223.

4. Lin, S., Owald, D., Chandra, V., Talbot, C., Huetteroth, W., and Waddell, S. (2014). Neural correlates of water reward in thirsty Drosophila. Nat. Neurosci. *17*, 1536–1542. https://doi.org/10.1038/nn.3827.

5. Duistermars, B.J., Chow, D.M., and Frye, M.A. (2009). Flies require bilateral sensory input to track odor gradients in flight. Curr. Biol. *19*, 1301–1307. https://doi.org/10.1016/j.cub.2009.06.022.

6. Krishnan, P., Duistermars, B.J., and Frye, M.A. (2011). Odor identity influences tracking of temporally patterned plumes in Drosophila. BMC Neurosci. *12*, 62. https://doi.org/10.1186/1471-2202-12-62.

7. Wasserman, S., Lu, P., Aptekar, J.W., and Frye, M.A. (2012). Flies dynamically anti-track, rather than ballistically escape, aversive odor during flight. J. Exp. Biol. *215*, 2833–2840. https://doi.org/10.1242/jeb.072082.

8. Ji, F., and Zhu, Y. (2015). A novel assay reveals hygrotactic behavior in Drosophila. PLoS One *10*, e0119162. https://doi.org/10.1371/journal.pone.0119162.

9. Perttunen, V., and Erkkilä, H. (1952). Humidity reaction in Drosophila melanogaster. Nature *169*, 78. https://doi.org/10.1038/169078a0.

10. Matzkin, L.M., Watts, T.D., and Markow, T.A. (2009). Evolution of stress resistance in Drosophila: interspecific variation in tolerance to desiccation and starvation. Funct. Ecol. *23*, 521–527. https://doi.org/10.1111/j.1365-2435.2008.01533.x.

11. Niveditha, S., Deepashree, S., Ramesh, S.R., and Shivanandappa, T. (2017). Sex differences in oxidative stress resistance in relation to longevity in Drosophila melanogaster. J. Comp. Physiol. B *187*, 899–909. https://doi.org/10.1007/s00360-017-1061-1.

12. Kristensen, T.N., Loeschcke, V., Tan, Q., Pertoldi, C., and Mengel-From, J. (2019). Sex and age specific reduction in stress resistance and mitochondrial DNA copy number in Drosophila melanogaster. Sci. Rep. *9*, 12305. https://doi.org/10.1038/s41598-019-48752-7.

13. Lin, Y.-J., Seroude, L., and Benzer, S. (1998). Extended life-span and stress resistance in the Drosophila mutant methuselah. Science *282*, 943–946. https://doi.org/10.1126/science.282.5390.943.

14. Batschelet, E. (1981). Circular Statistics in Biology (ACADEMIC PRESS).

15. Goldberg, J.M., and Brown, P.B. (1969). Response of binaural neurons of dog superior olivary complex to dichotic tonal stimuli: some physiological mechanisms of sound localization. J. Neurophysiol. *32*, 613–636. https://journals.physiology.org/doi/abs/10.1152/jn.1969.32.4.613.

16. Lau, M.-T., Lin, Y.Q., Kisling, S., Cotterell, J., Wilson, Y.A., Wang, Q.-P., Khuong, T.M., Bakhshi, N., Cole, T.A., Oyston, L.J., et al. (2017). A simple high throughput assay to evaluate water consumption in the fruit fly. Sci. Rep. *7*, 16786. https://doi.org/10.1038/s41598-017-16849-6.

17. Ja, W.W., Carvalho, G.B., Zid, B.M., Mak, E.M., Brummel, T., and Benzer, S. (2009). Water- and nutrient-dependent effects of dietary restriction on Drosophila lifespan. Proc. Natl. Acad. Sci. USA *106*, 18633–18637. https://doi.org/10.1073/pnas.0908016106.

18. Fanson, B.G., Yap, S., and Taylor, P.W. (2012). Geometry of compensatory feeding and water consumption in Drosophila melanogaster. J. Exp. Biol. *215*, 766–773. https://doi.org/10.1242/jeb.066860.

19. Duistermars, B.J., Care, R.A., and Frye, M.A. (2012). Binocular interactions underlying the classic optomotor responses of flying flies. Front. Behav. Neurosci. *6*, 6. https://doi.org/10.3389/fnbeh.2012.00006.

20. Mongeau, J.-M., and Frye, M.A. (2017). Drosophila spatiotemporally integrates visual signals to control saccades. Curr. Biol. *27*, 2901–2914.e2. https://doi.org/10.1016/j.cub.2017.08.035.

21. Van Breugel, F., and Dickinson, M.H. (2014). Plume-tracking behavior of flying drosophila emerges from a set of distinct sensory-motor reflexes. Curr. Biol. *24*, 274–286. https://doi.org/10.1016/j.cub.2013.12.023.

22. Clements, A.N. (1999). The biology of mosquitoes. Volume 2: sensory reception and behaviour (CABI publishing).

23. Leitch, K.J., Ponce, F.V., Dickson, W.B., van Breugel, F., and Dickinson, M.H. (2021). The long-distance flight behavior of Drosophila supports an agent-based model for wind-assisted dispersal in insects. Proc. Natl. Acad. Sci. USA *118*. e2013342118. https://doi.org/10.1073/pnas.2013342118.

24. Li, S., Li, B., Gao, L., Wang, J., and Yan, Z. (2022). Humidity response in Drosophila olfactory sensory neurons requires the mechanosensitive channel TMEM63. Nat. Commun. *13*, 3814. https://doi.org/10.1038/s41467-022-31253-z.

25. Frank, D.D., Enjin, A., Jouandet, G.C., Zaharieva, E.E., Para, A., Stensmyr, M.C., and Gallio, M. (2017). Early integration of temperature and humidity stimuli in the Drosophila brain. Curr. Biol. *27*, 2381–2388.e4. https://doi.org/10.1016/j.cub.2017.06.077.

26. Knecht, Z.A., Silbering, A.F., Cruz, J., Yang, L., Croset, V., Benton, R., and Garrity, P.A. (2017). Ionotropic receptor-dependent moist and dry cells control hygrosensation in

Drosophila. Elife *6*, e26654. https://doi.org/10.7554/eLife.26654.

27. Knecht, Z.A., Silbering, A.F., Ni, L., Klein, M., Budelli, G., Bell, R., Abuin, L., Ferrer, A.J., Samuel, A.D., Benton, R., et al. (2016). Distinct combinations of variant ionotropic glutamate receptors mediate thermosensation and hygrosensation in drosophila. Elife *5*, e17879. https://doi.org/10.7554/eLife.17879.

28. Enjin, A., Zaharieva, E.E., Frank, D.D., Mansourian, S., Suh, G.S.B., Gallio, M., and Stensmyr, M.C. (2016). Humidity sensing in drosophila. Curr. Biol. *26*, 1352–1358. https://doi.org/10.1016/j.cub.2016.03.049.

29. Marin, E.C., Büld, L., Theiss, M., Sarkissian, T., Roberts, R.J.V., Turnbull, R., Tamimi, I.F.M., Pleijzier, M.W., Laursen, W.J., Drummond, N., et al. (2020). Connectomics analysis reveals first-second-and third-order thermosensory and hygrosensory neurons in the adult Drosophila brain. Curr. Biol. *30*, 3167–3182.e4. https://doi.org/10.1016/j.cub.2020.06.028.

30. Vosshall, L.B., and Hansson, B.S. (2011). Unified nomenclature system for the insect olfactory coreceptor. Chem. Sens. *36*, 497–498. https://academic.oup.com/chemse/article/36/6/497/479049?login=true.

31. Wasserman, S., Salomon, A., and Frye, M.A. (2013). Drosophila tracks carbon dioxide in flight. Curr. Biol. *23*, 301–306. https://doi.org/10.1016/j.cub.2012.12.038.

32. von Arx, M., Goyret, J., Davidowitz, G., and Raguso, R.A. (2012). Floral humidity as a reliable sensory cue for profitability assessment by nectar-foraging hawkmoths. Proc. Natl. Acad. Sci. USA *109*, 9471–9476. https://doi.org/10.1073/pnas.1121624109.

33. von Arx, M. (2013). Floral humidity and other indicators of energy rewards in pollination biology. Commun. Integr. Biol. *6*, e22750. https://doi.org/10.4161/cib.22750.

34. Dahake, A., Jain, P., Vogt, C., Kandalaft, W., Stroock, A., and Raguso, R.A. (2022). Floral humidity as a signal – not a cue – in a nocturnal pollination system. Preprint at bioRxiv. https://doi.org/10.1101/2022.04.27.489805.

35. Harrison, A.S., and Rands, S.A. (2021). The ability of bumblebees Bombus terrestris (Hymenoptera: Apidae) to detect floral humidity is dependent upon environmental humidity. Preprint at bioRxiv. https://doi.org/10.1101/2021.08.13.456254.

36. Sengupta, P. (2013). The belly rules the nose: feeding state-dependent modulation of peripheral chemosensory responses. Curr. Opin. Neurobiol. *23*, 68–75. https://doi.org/10.1016/j.conb.2012.08.001.

37. Suver, M.P., Mamiya, A., and Dickinson, M.H. (2012). Octopamine neurons mediate flight-induced modulation of visual processing in Drosophila. Curr. Biol. *22*, 2294–2302. https://doi.org/10.1016/j.cub.2012.10.034.

38. Jang, H., Kim, K., Neal, S.J., Macosko, E., Kim, D., Butcher, R.A., Zeiger, D.M., Bargmann, C.I., and Sengupta, P. (2012). Neuromodulatory state and sex specify alternative behaviors through antagonistic synaptic pathways in C. elegans. Neuron *75*, 585–592. https://doi.org/10.1016/j.neuron.2012.06.034.

39. Gáliková, M., Dircksen, H., and Nässel, D.R. (2018). The thirsty fly: ion transport peptide (ITP) is a novel endocrine regulator of water homeostasis in Drosophila. PLoS Genet. *14*, e1007618. https://doi.org/10.1371/journal.pgen.1007618.

40. Kanwal, J.K., Coddington, E., Frazer, R., Limbania, D., Turner, G., Davila, K.J., Givens, M.A., Williams, V., Datta, S.R., and Wasserman, S. (2021). Internal state: dynamic, interconnected communication loops distributed across body, brain, and time. Integr. Comp. Biol. *61*, 867–886. https://doi.org/10.1093/icb/icab101.

41. Berntson, G.G., and Khalsa, S.S. (2021). Neural circuits of interoception. Trends Neurosci. *44*, 17–28. https://doi.org/10.1016/j.tins.2020.09.011.

42. Petzschner, F.H., Garfinkel, S.N., Paulus, M.P., Koch, C., and Khalsa, S.S. (2021). Computational models of interoception and body regulation. Trends Neurosci. *44*, 63–76. https://doi.org/10.1016/j.tins.2020.09.012.

43. Chen, W.G., Schloesser, D., Arensdorf, A.M., Simmons, J.M., Cui, C., Valentino, R., Gnadt, J.W., Nielsen, L., Hillaire-Clarke, C.S., Spruance, V., et al. (2021). The emerging science of interoception: sensing, integrating, interpreting, and regulating signals within the self. Trends Neurosci. *44*, 3–16. https://doi.org/10.1016/j.tins.2020.10.007.

44. Maimon, G., Straw, A.D., and Dickinson, M.H. (2008). Report A simple vision-based algorithm for decision making in flying Drosophila. Curr. Biol. *18*, 464–470. https://doi.org/10.1016/j.cub.2008.02.054.

45. Frye, M.A., and Duistermars, B.J. (2009). Visually mediated odor tracking during flight in Drosophila. J. Vis. Exp. e1110. https://doi.org/10.3791/1110.

46. Bender, J. a, and Dickinson, M.H. (2006). Visual stimulation of saccades in magnetically tethered Drosophila. J. Exp. Biol. *209*, 3170–3182. https://doi.org/10.1242/jeb.02369.

47. Berens, P. (2009). CircStat: a MATLAB toolbox for circular statistics. J. Stat. Softw. *31*, 1–21. https://doi.org/10.18637/jss.v031.i10.

STAR★METHODS

KEY RESOURCES TABLE

REAGENT or RESOURCE	SOURCE	IDENTIFIER
Deposited data		
Heading trajectory angle files	This paper https://figshare.com	Figshare: https://doi.org/10.6084/m9.figshare.20387544
Data frames	This paper https://figshare.com	Figshare: https://doi.org/10.6084/m9.figshare.20387535
Experimental and Analysis Code	This paper https://figshare.com	Figshare: https://doi.org/10.6084/m9.figshare.20387580
Software and algorithms		
MATLAB	Mathworks	https://www.mathworks.com/products/matlab.html

RESOURCE AVAILABILITY

Lead contact

Further information and requests for resources should be directed to and will be fulfilled by the Lead Contact, Sara Wasserman (swasserm@wellesley.edu).

Materials availability

This study did not generate new unique reagents.

Data and code availability

- All plume tracking data have been deposited at figshare.com and are publicly available as of the date of publication. DOIs are listed in the key resources table.
- All original code has been deposited at figshare.com and is publicly available as of the date of publication. DOIs are listed in the key resources table.
- Any additional information required to reanalyze the data reported in this paper is available from the lead contact upon request.

EXPERIMENTAL MODEL AND SUBJECT DETAILS

Wild type flies, *D. Melanogaster* (Meigen), have been reared in a lab setting for more than ten years. *Orco*$^{-/-}$ mutants were kindly provided by the Vosshall Lab via the Garrity Lab. Ir68-GAL4 (w[1118]; Sp/CyO; Ir68a [3xp3-RFP-T2A-Gal4]/TM6B, Hu) were graciously provided by the Garrity Lab and backcrossed to insert wild-type copy for red eyes (w+; +;Ir68aGal4). Empty-GAL4 (w[1118]; P{y[+t7.7] w[+mC] = GAL4.1Uw} attP2; BDSC 68384) and UAS-Kir (w[1118]; P{y[+t7.7] w[+mC] = GAL4.1Uw}attP2; kindly provided by the Dickinson Lab). All flies were fed a standard cornmeal and molasses diet and were maintained under a 12 h:12 h light:dark cycle at 25°C. Female flies used were 3–6 days post-eclosion. Flies in the acute dehydration condition were removed from food and water for 3 h total before they were run in any given experiment. Flies in the time point experiments were tethered only for 30 min and then run at the 1st, 2nd, and 3rd hour mark after they were removed from food and water. Starved and hydrated flies were placed in a vial with 1% non-nutritional agarose (SIGMA, Type II: Medium EEO,[17]) and placed in the arena within the time frame indicated. Random individuals were chosen for each experiment and no experimenter blinding was done. N values can be found in each figure legend.

METHOD DETAILS

Magnetic tether flight simulator

A magnetic tether arena with an odor delivery system has been previously described.[1,2,6,44,45] Briefly, flies were cold anesthetized and tethered to minutien pins (Fine Science Tools, 26002-20) using UV glue (Plas-Pak Industries) cured with a UV light gun (LED 200, Electro-Lite). The flies were suspended between two rare-earth magnets which allowed for the free rotation of the flies along the yaw axis. A visual panel of

blue (470 nm) LEDs surrounded the fly in azimuth and reached 60° above and below the visual horizon. The flies were illuminated with infrared LEDs (Adafruit Super-bright 5 mm IR, 940 nm) and recorded using a Firefly_MV_FFMV_03M2M and Point Grey FlyVCap2 software, and the Point Grey MATLAB toolbox.

Water and Apple Cider Vinegar (ACV) plumes were delivered to the arena using a multiplexer regulated by a mass-flow system (Sable Systems) set at a rate of 12 mL/min through a test tube containing either 1.5 mL of Deionized water, 1.5 mL of apple cider vinegar (ACV, Ralph's grocery brand), or a filter paper with 25 μL of ACV. The plume is 20° wide and is indicated in figures by a blue or green rectangle to denote the water or apple cider vinegar (ACV) plume, respectively. Plume dynamics and odor intensity profile have been previously characterized.[31] The odorants passed through non-adsorbing PTFE tubing (Zeus) and were replaced between experiments. The plume was placed in the arena at 180°, 4 mm above the head of the fly, and 10 mm from the top of a vacuum set to 10 L/min (flow regulator used, Cole Parmer Instruments) placed beneath the fly to keep the odor concentrated in a specific part of the arena. Humidity and temperature at the sides of the arena and in the room were measured using a Traceable Thermohygrometer with Calibration (Cole Parmer). The average temperature of the room was 23°C and the relative humidity (RH) was 38%. The temperature and RH of the various sides of the arena were measured four times with 30 min intervals between them. The average temperature inside the arena was 25°C and the RH was 41% at the plume side, 35% at the opposite side of the plume, and 35% at the top and bottom of the arena. Next, the relative humidity of some environmental locations was measured. The RH at the top of an exterior plant and a compost pile at dusk was found to be 62% with an ambient RH of 55% and 54%, respectively. All experiments started with continuous rotation of a 20° vertical black bar around a uniform background for 20 s, to ensure that all flies could rotate freely. In order to decrease the number of flies beginning the trial heading into the plume, the bar oscillated at 90° from the nozzle for 8 s to activate the frontal fixation response and bring the fly to a starting position. Flies that did not start at 90° were likely to start at 270° and were still included in the analysis. Four conditions were randomly presented to the fly. After the oscillating bar was switched off, a static striped visual grating (30° spatial wavelength) background was presented to the fly and paired either with the water or ACV odorant for 25 s. For any experiment, each fly was run for a minimum of two and maximum of three trials, and trials were excluded if the fly stopped flying more than three times. A thin layer of UV-activated glue was painted over the third antennal segment for the antennal occlusions (AO) experiments.[5,31]

All data analysis was performed using custom-written MATLAB software. The probability of finding the flies heading towards the plume was calculated by dividing the sum of the frames spent in the plume (+/− 20° envelope around the nozzle). All analyses were done on the last 20-s of the 25-s trial except for the Two-sample Kolmogorov-Smirnov test which included the entire 25-s trial.

Saccades were defined as previously reported.[20] Briefly, noise levels were calculated in the presence of spikes in velocity and used to determine the threshold of a saccade as being at least four times the noise level. The peak of a spike in velocity was determined by computing the local maxima while the duration of a saccade was found by measuring the time when the angular velocity was greater than one-quarter of the peak amplitude.[46] Termination of a saccade was determined as one-quarter of the peak angular velocity. Finally, saccades were included in analysis if their amplitude fell between 11° and 175°.

QUANTIFICATION AND STATISTICAL ANALYSIS

Two-sample unpaired t-tests or one-way ANOVA followed by a Bonferroni post hoc test were used to compare the probability of finding the flies in the plume and to compare saccade dynamics. Two-sample Kolmogorov-Smirnov tests were used to compare heading distributions. Heading variance over time was compared by vector strength.[14,15] Vector strength was calculated using the Circular Statistics Toolbox[47] in MATLAB by calculating the circular r strength of the flies per frame. Saccade number was compared via Mann Whitney U Test. All other statistical analyses were performed using the MATLAB statistics toolbox.